JOURNAL OF PHYSIOLOGY AND PHARMACOLOGY 2017, 68, 3, 385-395
www.jpp.krakow.pl

A.F. DEFTU[1], A. FILIPPI[1, 2], K. SHIBASAKI[3], R.O. GHEORGHE[1], M. CHIRITOIU[4], V. RISTOIU[1]

CHEMOKINE (C-X-C MOTIF) LIGAND 1 (CXCL1) AND CHEMOKINE (C-X-C MOTIF) LIGAND 2 (CXCL2) MODULATE THE ACTIVITY OF TRPV1+/IB4+ CULTURED RAT DORSAL ROOT GANGLIA NEURONS UPON SHORT-TERM AND ACUTE APPLICATION

[1]Department of Anatomy, Animal Physiology and Biophysics, Faculty of Biology, University of Bucharest, Bucharest, Romania;
[2]Department of Medical Biophysics, University of Medicine and Pharmacy 'Carol Davila', Bucharest, Romania;
[3]Department of Molecular and Cellular Neurobiology, Gunma University Graduate School of Medicine, Maebashi, Japan;
[4]Department of Molecular Cell Biology, Institute of Biochemistry, Romanian Academy, Bucharest, Romania

CXCL1 and CXCL2 are two chemokines with 78% homology of their sequence. CXCL1 was associated with atopic dermatitis, a highly pruritic skin disease, but it is not clear what is its mechanism of action, while for CXCL2 there are no data about an association with itch sensitivity. CXCL1 and CXCL2 can modulate TRPV1 receptors, which are one of the most important downstream effectors for itch sensitivity, upon short-term (4 h) or long-term (24 h) incubation, but the data are incomplete. Therefore, the aims of this study were to better characterize the short-term effects of CXCL1 and CXCL2 on TRPV1$^+$/IB4$^+$ dorsal root ganglia neurons known to include nociceptor and itch-sensitive neurons, and to obtain new data about the acute application (12 min) of the two chemokines on the same population of neurons. The results showed that 4 nM CXCL1 and 3.6 nM CXCL2 significantly reduce TRPV1 desensitization in TRPV1$^+$/IB4$^+$ DRG neurons after short-term incubation, but when acutely applied CXCL1 activated a sub-population of itch-sensitive TRPV1$^+$/IB4$^+$ cells in a slow, low amplitude manner, while CXCL2 had a similar effect but on non-itch TRPV1$^+$/IB4$^+$ DRG neurons. These data contribute to a better understanding of CXCL1 and CXCL2 mechanism of action for both pain and itch inducing effects.

Key words: *chemokine (C-X-C motif) ligand 1, chemokine (C-X-C motif) ligand 2, transient receptor potential vanilloid type 1, isolectin B4, dorsal root ganglia neurons, pain, itch*

INTRODUCTION

Chemokine (C-X-C motif) ligand 1 (CXCL1) and chemokine (C-X-C motif) ligand 2 (CXCL2) are two low-molecular-weight members of the ELR(+) CXC chemokine family with 78% homology of their sequence (1), which act specifically through CXCR2, a G protein-coupled receptor (2). Both of them are known to have pleiotropic effects on neurons or immune cells, ranging from stimulating proliferation to increasing pain (3). In addition, CXCL1 was associated with atopic dermatitis, a highly pruritic skin disease (4, 5), but it is not clear what is its mechanism of action. In contrast, for CXCL2 there are no data about an association with itch sensitivity.

Itch (pruritus) defined as 'an unpleasant sensation that elicits the desire or reflex to scratch' (6), it is evoked mainly from the skin and implicates activation of a specific subset of isolectin B4 (IB4$^+$), C-type primary afferents that respond directly to itch-producing agents or are activated indirectly by mast cells, keratinocytes or fibroblasts that release itch-producing compounds (7). These fibers use different molecular pathways to transduce itch, with transient receptor potential vanilloid type 1 (TRPV1) and transient receptor potential channel, subfamily A member 1 (TRPA1) receptors found to be the most important downstream effectors (8-10). Specifically, TRPV1 receptors are important in mediating histamine-induced itch in ~23 – 29% of IB4$^+$ mice dorsal root ganglia (DRG) neurons *via* H1 histamine receptors and PLCβ3 (11) or PKCδ (12). TRPA1 receptors mediate histamine-independent itch to chloroquine and BAM8-22 (bovine adrenal medulla 8-22) peptide in ~3 – 5% of TRPV1$^+$/TRPA1$^+$/IB4$^+$ histamine-sensitive mice DRG neurons *via* MrgprA3 (Mas-related G-protein coupled) and MrgprC11 receptors (9, 13, 14), and both TRPA1 and TRPV1 receptors mediate IL-31-induced itch in ~4% of TRPV1$^+$/TRPA1$^+$ DRG neurons (15). At acute application, histamine evokes a TRPV1 response of low amplitude and slow kinetics (~100 s duration) (16), while chloroquine has no effect on TRPV1, but robustly activates TRPA1 (9).

TRPV1 is a polymodal, non-selective cation channel that is specifically expressed in a subset of somatosensory neurons located in the dorsal root and trigeminal ganglia. It is directly activated by capsaicin, protons, heat and by endogenous or exogenous agonists of natural, semisynthetic and synthetic origin (17, 18). According to the existing data, CXCL1 and CXCL2 can also modulate TRPV1 activity. More precisely, short-term incubation (4 h) with 1.5 nM CXCL1 can reduce TRPV1 desensitization but it has no effect on the amplitude of

TRPV1 response (19), while long-term incubation (24 h) at the same concentration has no effect neither on the amplitude of TRPV1 response, nor on its desensitization (3). For CXCL2 there are no data on any effect on TRPV1 receptors after short-term incubation, but we have shown that long-term incubation with 1.5 nM can significantly decrease the TRPV1 current and increase its desensitization rate (3). Knowing that these two chemokines share a 78% homology (1), it is rather surprising that they have opposite effects, especially on long-term incubation where there are available data for both of them.

To better understand how these two chemokines act and to investigate if they activate the itch-sensitive DRG neurons, in this study we tested: 1) the effect of short-term incubation with CXCL2 on the TRPV1 rate of desensitization to see whether CXCL2 can still affect TRPV1 receptors in the same manner as CXCL1, and 2) what would be the effect of acute application of CXCL1 or CXCL2. In contrast to previous studies in which CXCL1 and CXCL2 effects were investigated in all $TRPV1^+$ DRG neurons, in our study we focused only on $TRPV1^+/IB4^+$ DRG neurons to which the itch-sensitive neurons belong.

MATERIALS AND METHODS

Animals

For this study, 80 adult male Wistar rats (100 – 150 g) from the animal facility of the 'Ion Cantacuzino' National Institute, Bucharest, Romania were used. All procedures were carried out in accordance with the Directive 2010/63/EU revising Directive 86/609/EEC on the protection of animals used for scientific purposes and were approved by the Bioethics Committee of the Faculty of Biology, University of Bucharest and Graduate School of Medicine, Gunma University.

Cell culture

Rats were killed by inhalation of 100% CO_2 followed by decapitation. DRG from all spinal segments were removed and prepared for the cell culture as previously described (20). Briefly, neurons were dissociated in 1 mg/ml collagenase IA and 2 mg/ml dispase (Gibco, 17105041) for 1 hour at 37°C, then plated on 13 mm glass coverslips pretreated with poly-D-lysine (0.1 mg/ml for 30 min) and cultured in a NGF-free 1:1 mixture of 7.4 mM glucose DMEM and Hams's F10 medium with 10% horse serum, 0.5% penicillin/streptomycin and 1% L-glutamine (Thermo Fisher Scientific, A1286001) at 37°C, in 5% CO_2 in air. Human embryonic kidney cells (HEK293T) cultured according to an existing protocol (20), were transiently transfected with 1 µg/µl of huCXCR2 (kindly donated by Dr. Ann Richmond, Vanderbilt University, TN, USA) using Lipofectamine 2000 (Life Technologies). If not otherwise specified, all reagents were from Sigma. Experiments were conducted at room temperature (25°C), 24 hours after plating the cells.

Intracellular Ca^{2+} imaging

Cells cultured on coverslips were incubated for 30 minutes at 37°C in standard extracellular solution (see *Solutions* below) containing 2 µM Calcium Green-1 AM and 0.02% Pluronic F-127 (both from Invitrogen), and left to recover for 30 minutes before use. Coverslips were mounted in a Teflon chamber (RC-40HP, Harvard Apparatus, USA) on the stage of an Eclipse TE300 inverted microscope (Nikon, Japan) and left for 5 minutes to adapt to the extracellular solution flow at 25°C. Neurons were illuminated with an Optoscan monocromator (Cairn Instruments, UK) and the fluorescence changes were captured with a 12-bit CCD SensiCam camera (PCO, Germany). The data were recorded using Axon Imaging Workbench 4.0 (Indec Biosystems, USA). After background subtraction, data were quantified as $\Delta F/F0$ for each recorded cell, representing the ratio between the maximum fluorescence change during the stimulus and the baseline fluorescence before the stimulus.

To define capsaicin sensitivity, a histogram of all responses ($\Delta F/F0$) was fitted with a two-peak Gaussian and the cutoff value was taken as the mean ± 2 SD of the Gaussian peak centered closest to zero. The cells which responded to capsaicin application with a $\Delta F/F0 \geq 0.1$ were considered capsaicin-sensitive.

To investigate the effect of short-term incubation of CXCL2 on TRPV1 responses, we used the same time interval as previously published, i.e. 4 h (19). In addition, because in the above mentioned studies it was used only one concentration for both CXCL1 and CXCL2 (i.e. 1.5 nM), we decided to test several concentrations of CXCL2 ranging from 0.06 to 40.5 nM, in an increment with a factor of 3 which thus also included the 1.5 nM concentration, in order to identify the most appropriate concentration (EC_{50}) to generate a response. We did this for CXCL1 to get more data about this chemokine as well.

To identify the non-peptidergic $IB4^+$ neurons (21), isolectin B4 (IB4) conjugated with fluorescein isothiocyante (FITC) (3 µg/ml, Sigma, L2895) was added to the extracellular solution for 10 minutes at the end of the recording. To avoid interference between excitation wavelengths (Calcium green, λ_{ex}= 506 nm and IB4-FITC, λ_{ex}= 490 nm), images of the field of cells taken before and after IB4-FITC application were merged in Image-J software (version 1.37, Wayne Rasband, NIH, Bethesda, MD, USA) after pseudo-colors were associated to them (*Fig. 1*).

The recording protocol was the following: after 4 hours incubation with different concentrations of CXCL1 or CXCL2, TRPV1 responses elicited by two consecutive 250 nM capsaicin applications of 20 s duration at 10 min interval was followed by a short application (10 s) of 50 mM KCl to evaluate if the responsive cells are viable neurons and by the IB4-FITC staining as mentioned above. To analyze the effect on the rate of desensitization induced by repeated application of capsaicin, the fluorescence change ratio between the second capsaicin application and the first one ($\Delta F/F0_{2nd}/\Delta F/F0_{1st}$) was determined.

To investigate the effect of acute application of CXCL1 or CXCL2 on $TRPV1^+/IB4^+$ DRG neurons, the two chemokines were applied for 12 minutes at the EC_{50} calculated in the previous experiments, followed by 20 s application of 250 nM capsaicin to test if indeed the cells were $TRPV1^+$ and as above, by the 50 nM KCl application and IB4-FITC staining. The application time was selected because according to preliminary studies, this time was enough for a full recovery of the fluorescence change. Cells were judged to be responsive if the $\Delta F/F0$ ratio value increased by greater than 10% of the resting level after chemical application.

Immunocytochemistry (ICC)

Cells cultured on coverslips were fixed in 4% paraformaldehyde (PFA) solution (Roth) in 0.01 M phosphate buffer (PBS) for 20 minutes, permeabilized with a 0.3% Triton X-100 solution in PBS for 15 minutes and incubated for 1 hour in blocking solution (0.3% Triton X-100 and 4% normal goat serum in PBS). After overnight incubation at 4°C with the primary antibodies, cells were washed, incubated for 1 hour with the secondary antibodies and cover-slipped with Prolong Gold antifade (Life Technologies). The slides were visualized

under an AxioObserver D1 Zeiss (Carl Zeiss, Germany) fluorescence microscope and processed with Image-J software. The primary antibodies were biotinylated isolectin B4 (1:200, Vector Laboratories, B-1205), anti-βIII-tubulin (1:4000, mouse monoclonal, Abcam, 78078), anti-CXCR2 (1:200, rabbit polyclonal, Santa-Cruz Biotechnology, sc-682) and anti-TRPV1 (1:100, rabbit polyclonal, Santa-Cruz Biotechnology, sc-28759). The secondary antibodies were (from Life Technologies) Streptavidin-Alexa Fluor 488 Conjugate (1:1500, S32354), goat anti-rabbit Alexa Fluor 568 (1:1500, A11011) and goat anti-mouse Alexa Fluor 568 (1:1500, A11004).

Western blotting

Cultured DRG neurons and HEK293T cells were lysed in RIPA (1% NP40) buffer as previously described (22). The extracted proteins were separated on 8% SDS-PAGE, transferred on nitrocellulose and probed with rabbit anti-CXCR2 (1:300, Santa-Cruz Biotechnology, sc-682) and rabbit anti-α-tubulin (1:10000, Abcam, ab18251) antibodies. The secondary antibodies were goat anti-α-rabbit coupled with HRP (horse radish peroxidase) (1:10,000, Santa-Cruz Biotechnology, sc-2004). Visualization was made with Pierce ECL Western blotting substrate (Thermo Scientific, 32106). For EndoH (NEB) (NEB, UK, P0702S,) digestion which removes sugar residues from proteins, the whole lysates were denatured for 5 minutes at 100°C in denaturating buffer containing 0.5% SDS and 40 mM DTT, then cooled and mixed with 1/10 EndoH reaction buffer (0.5 M sodium citrate, pH 5.5). EndoH (250 units) was added to one-half of the sample, whereas the other half contained EndoH buffer alone. All samples were incubated for 18 hours at 37°C and used for SDS-PAGE and Western blotting as previously described. If not otherwise mentioned, all the other reagents were from Santa Cruz Biotechnology.

Scratch test

To measure itch-related behavior, 20 µl of 10 µM CXCL1 was injected into the neck intradermally. Bouts of scratching with the hindpaw directed towards the injection site were counted for 30 minutes as previously described (23). Capsazepine, a TRPV1 antagonist (20 µl, 10 mM) and HC067047, a TRPV4 antagonist (20 µl, 10 mM) were pre-injected 15 minutes before the CXCL1 challenge.

Solutions

Standard extracellular solution (ES) contained (in mM): NaCl 140, KCl 4, $MgCl_2$ 1, $CaCl_2$ 2, HEPES 10, NaOH 4.54, glucose 7.4, pH = 7.4 at 25°C. Drugs were added from the stock solutions prepared in deionized water for CXCL1, 10 µM and CXCL2, 5 µM both from Promokine, Germany, and in ethanol for capsaicin 1 mM. If not otherwise mentioned, all the reagents were from Sigma. The stock solutions were stored at –20°C and diluted to desired final concentration in ES in the day of the experiment.

Data analysis

Analysis was performed using AIW4 (INDEC BioSystems, USA), Microsoft Excel 2007 (Microsoft, USA), Prism 5.01 (GraphPad Software Inc., USA) and a macro program written by Liviu Soltuzu in Microsoft Excel 2007. All data were given as means ± S.E.M.; statistical significance was tested using 1 way ANOVA with Bonferonni post-test or Fisher's exact test. A value of $P < 0.05$ was considered to be statistically significant.

RESULTS

CXCL2 reduces TRPV1 desensitization in IB4⁺ neurons in the same nanomolar range as CXCL1

After 4 hours of incubation with different concentrations of CXCL1 and CXCL2 ranging from 0.06 to 40.5 nM, TRPV1 receptors were activated by two consecutive 250 nM capsaicin applications of 20 s duration at 10 minutes interval. The results showed a significant dose-dependent reduction of the TRPV1 rate of desensitization compared to control starting at 4.5 nM for both chemokines (*Fig. 2a* and *2b*; see also *Table 1*). From the concentration-response curve obtained by plotting normalized to control fluorescence change ratios against $\log_{10}$[CXCL1] or $\log_{10}$[CXCL2] to which a logistic dose-response function was fitted (*Fig. 2c, 2d* and insets), there were determined an EC_{50} of 4.0 nM ($\log EC_{50} = 0.61 \pm 0.24$) with a Hill slope of 1.19 ± 0.74 for CXCL1 and an EC_{50} of 3.6 nM ($\log EC_{50} = 0.56 \pm 0.34$) with a Hill slope of 1.56 ± 0.73 for CXCL2 (*Fig. 2c* and *2d*).

To confirm that there was no error in the identification of the IB4⁺ population possibly due to an overlapping between the excitation wavelengths of Calcium-green and the FITC bound to IB4, we compared the percentages of IB4⁺ cells in calcium experiments calculated versus the total population of cells, with the percentages in an ICC staining in which the IB4⁺ neurons were determined against the total neuronal population stained with βIII tubulin antibody, a specific neuronal marker (*Fig. 3a*). According to these data, the IB4⁺ neurons represented 53% in calcium imaging experiments ($n_{total} = 144$, $n_{IB4+} = 76$) and 50% in ICC experiments ($n_{total} = 157$, $n_{IB4+} = 79$) which is in agreement with existing data (21, 24) and confirm the fact that the IB4⁺ population was correctly identified.

As mentioned in the introduction, CXCL1 and CXCL2 act specifically through CXCR2, a G protein-coupled receptor (2). Therefore, we confirmed by Western blot the CXCR2 expression in the general population of DRG neurons (*Fig. 3d* and *3e*) and by ICC, we confirmed its expression in the IB4⁺ neurons similar to TRPV1 receptors (*Fig. 3b* and *3c*). Since according to ICC staining the CXCR2 receptors seem to be expressed in all DRG neurons, to eliminate the possibility of a non-specific binding, the antibody specificity was reconfirmed in HEK293T cells transiently transfected with CXCR2 plasmid (*Fig. 3f*) and in untransfected HEK293T cells (*Fig. 3g*). The results confirmed that indeed the antibody specifically detects CXCR2 receptors at the DRG neurons' level, and that these receptors are expressed by both IB4⁺ and IB4⁻ neurons.

Acute application of CXCL1 induced an $[Ca^{2+}]_i$ increase larger than the one induced by CXCL2, in a bigger population of dorsal root ganglion neurons

After establishing the EC_{50} concentration at which CXCL1 and CXCL2 can elicit a response from TRPV1 in the TRPV1⁺/IB4⁺ DRG neurons after short-term incubation, we also explored their acute application effects as described in the methods section. The EC_{50} values that we found are within the *in vitro* efficacy range according to the data in the literature: i.e. 1.28 – 12.8 nM for CXCL1 (25, 26) and 1.41 pM-12.8 nM for CXCL2 (27, 28). Therefore, even though the EC_{50} values were established after incubation experiments, we decided to use them for acute application experiments as well.

At acute application, 4 nM CXCL1 induced in only 23% ($n = 27$, $n_{total} = 116$) of TRPV1⁺/IB4⁺ DRG neurons an $[Ca^{2+}]_i$ increase with a slower kinetics than the one induced by capsaicin applied after washing CXCL1 and with an amplitude representing 46% of an independent capsaicin response (mean ΔF/F0 for CXCL1 = 0.37 ± 0.06, n = 27, mean ΔF/F0 for capsaicin = 0.80 ± 0.06, n =

24, *Fig. 4a* and *4c*). Acute application of 3.6 nM CXCL2 induced in only 5.4% (n = 12, n_{total} = 233) of TRPV1$^+$/IB4$^+$ DRG neurons an $[Ca^{2+}]_i$ increase with a slow kinetics, similar to CXCL1 (*Fig. 4a*), and with an amplitude representing 21% of an independent capsaicin response (mean ΔF/F0 for CXCL2 = 0.17 ± 0.02, n = 12, mean ΔF/F0 for capsaicin = 0.80 ± 0.06, n = 24), respectively 46% of the CXCL1 response (*Fig. 4c*). We chose to compare the amplitude of CXCL1- and CXCL2-induced responses with an independent capsaicin application to avoid any possible influences of the $[Ca^{2+}]_i$ increase induced by CXCL1 or CXCL2 on the subsequent capsaicin response. When the two chemokines were applied together, the $[Ca^{2+}]_i$ increase was elicited in 12% (n = 6, n_{total} = 49) of TRPV1$^+$/IB4$^+$ DRG neurons and represented 65% of the CXCL1-induced response (mean ΔF/F0 for CXCL1 + CXCL2 = 0.24 ± 0.04, n = 6, mean ΔF/F0 for CXCL1 = 0.37 ± 0.06, n = 27, *Fig. 4b* and *4c*).

CXCL1-sensitive TRPV1$^+$/IB4$^+$ dorsal root ganglion neurons also responded to itch-inducing agents

As mentioned above, the MrgprA3- or MrgprC11-positive mice DRG population defines a unique subset of capsaicin-sensitive, itch-specific neurons that respond to histamine, chloroquine and BAM8-22 peptide (13). To test if the CXCL1-sensitive or CXCL2-sensitive neurons belong to the itch-sensitive population, we investigated their responses to 100 s application of 100 µM histamine or 50 s application of 1 mM chloroquine applied at 4 minutes interval after CXCL1 or CXCL2 application and between them.

In the experiments using CXCL1, the itch-sensitive population, defined as histamine or chloroquine sensitive neurons, represented 39% (23/59) of all TRPV1$^+$/IB4$^+$ DRG neurons. In this population, 30% (7/23) neurons responded only to chloroquine, 26% (6/23) only to histamine, 17% (4/23) responded to histamine and chloroquine, 17% (4/23) to histamine, chloroquine and CXCL1, 4% (1/23) to histamine and CXCL1 and 4% (1/23) to chloroquine and CXCL1 (*Fig. 5a* and *5b*). Statistical analysis showed significant overlap between CXCL1 and histamine responsive neurons (Fisher's exact test, $P < 0.01$) and CXCL1 and chloroquine responsive neurons ($P < 0.01$), with CXCL1-sensitive neurons representing only a sub-population of the itch-sensitive neurons.

In the experiments using CXCL2, in the itch-sensitive population defined according to the same criteria as mentioned above, only 2% (1/48) of neurons responded to CXCL2, histamine and chloroquine, with no cells responding to CXCL2 and histamine or CXCL2 and chloroquine. Statistical analysis couldn't prove a significant overlap between CXCL2 responsive neurons and either histamine or chloroquine sensitive neurons (Fisher's exact test, $P > 0.05$), suggesting that the responses to

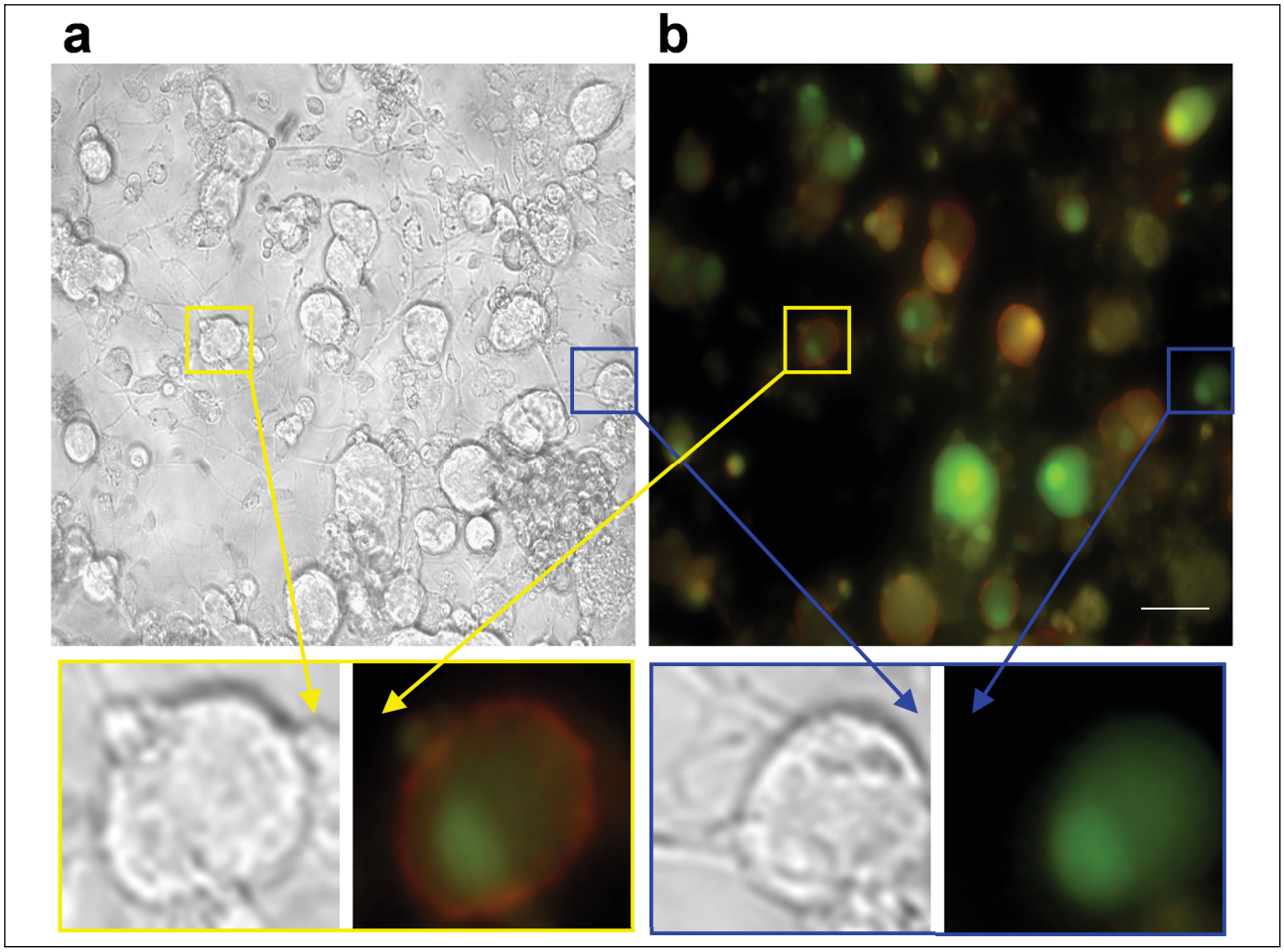

Fig. 1. Representative images of IB4$^+$ and IB4$^-$ dorsal root ganglia neurons. Image of a dorsal root ganglia culture under transmitted light (*a*) and after fluorescence excitation merged in Image-J software as described in the Methods section (*b*) (scale bar = 30 µm). The green signal corresponds to the loaded Calcium green, and the red signal indicates the IB4 staining. The insets in yellow frame indicate an IB4$^+$ cell, and the insets in blue frame indicate an IB4$^-$ cell.

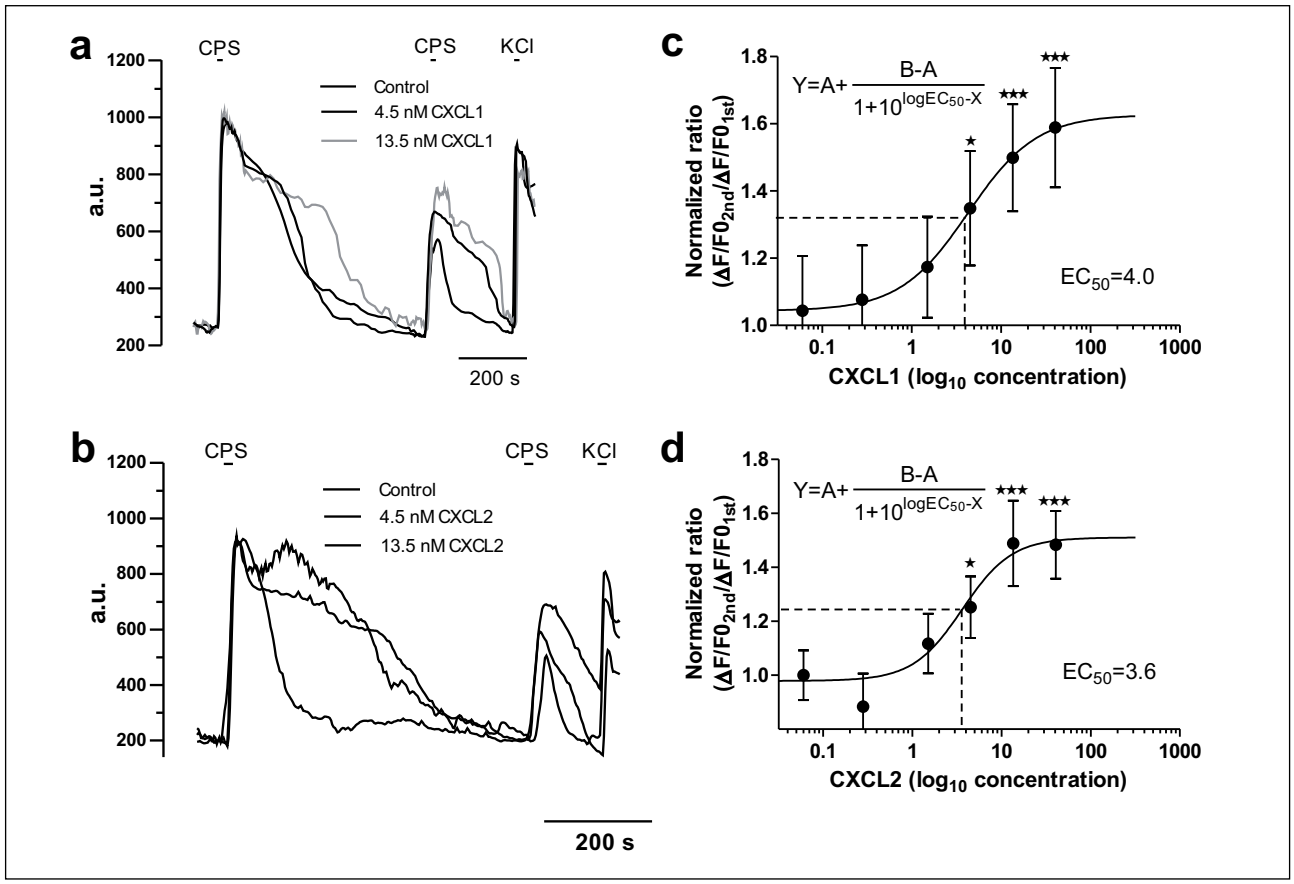

Fig. 2. Short-term incubation (4 h) with CXCL1 or CXCL2 reduced TRPV1 desensitization in IB4⁺ DRG neurons. (*a*) Representative traces of $[Ca^{2+}]_i$ in IB4⁺ neurons pre-incubated with CXCL1, after two consecutive 250 nM capsaicin applications. (*b*) Representative traces of $[Ca^{2+}]_i$ in IB4⁺ neurons pre-incubated with CXCL2, after two consecutive 250 nM capsaicin applications. (*c*) CXCL1 dose-dependently reduced TRPV1 desensitization with an EC_{50} of 4.0 nM as obtained by the logistic dose-response function (*inset*). (*d*) CXCL2 dose-dependently reduced TRPV1 desensitization with an EC_{50} of 3.6 nM as obtained by the logistic dose-response function (*inset*). For both CXCL1 and CXCL2, the $\Delta F/F0_{2nd}/\Delta F/F0_{1st}$ ratio was normalized to a similar ratio in untreated cells. CPS, capsaicin.

Table 1. Mean ratio of the fluorescence change ($\Delta F/F0_{2nd}/\Delta F/F0_{1st}$) induced by capsaicin-activated TRPV1 receptors in IB4⁺ dorsal root ganglia neurons.

Concentration (nM)	0 (control)	0.06	0.28	1.5	4.5	13.5	40.5
CXCL1	41.7 ± 3.73 (n = 60)	43.52 ± 5.56 (n = 26) P > 0.05	44.86 ± 5.42 (n = 25) P > 0.05	48.93 ± 4.48 (n = 41) P > 0.05	56.23 ± 5.01 (n = 45) $^{*}P < 0.05$	62.51 ± 3.59 (n = 51) $^{***}P < 0.001$	66.26 ± 4.45 (n = 20) $^{***}P < 0.001$
CXCL2	42.00 ± 2.73 (n = 106)	40.00 ± 4.14 (n = 36) P > 0.05	37.13 ± 4.54 (n = 28) P > 0.05	47.11 ± 3.59 (n = 40) P > 0.05	52.59 ± 3.35 (n = 31) $^{*}P < 0.05$	62.54 ± 5.26 (n = 33) $^{***}P < 0.001$	62.30 ± 3.36 (n = 45) $^{***}P < 0.001$

The statistical significance was obtained by comparing the mean ratio of the fluorescence change after pre-treatment with different concentrations of CXCL1, with similar values in control, untreated cells.

acute application of CXCL2 occur mainly in the non-itch TRPV1⁺/IB4⁺ DRG neurons.

Since these data suggested that CXCL1 plays a more important role in itch sensitivity than CXCL2, we subsequently investigated in behavioral tests only CXCL1. Given the fact that CXCL1-sensitive cells belong to TRPV1⁺/IB4⁺ cells, we tested if the CXCL1-induced itch upon intradermal injection was also sensitive to a TRPV1 blocking agent. The results showed that intradermal injection of CXCL1 induced strong scratching behavior (79.38 ± 2.19 bouts of scratching after CXCL1 (n = 8) compared to 32.38 ± 2.49 bouts of scratching (n = 8) after saline injection, $P < 0.001$), which was significantly reduced by 15 minutes capsazepine pre-treatment before CXCL1 (32.38 ± 2.49, n = 8, $P < 0.05$). HC067047 didn't have any significant effect (78.63 ± 3.38, n = 8, $P > 0.05$) (*Fig. 5c*).

DISCUSSION

In this study we showed that CXCL1 and CXCL2, two highly homologous chemokines, significantly reduce TRPV1 desensitization in TRPV1⁺/IB4⁺ DRG neurons after short-term

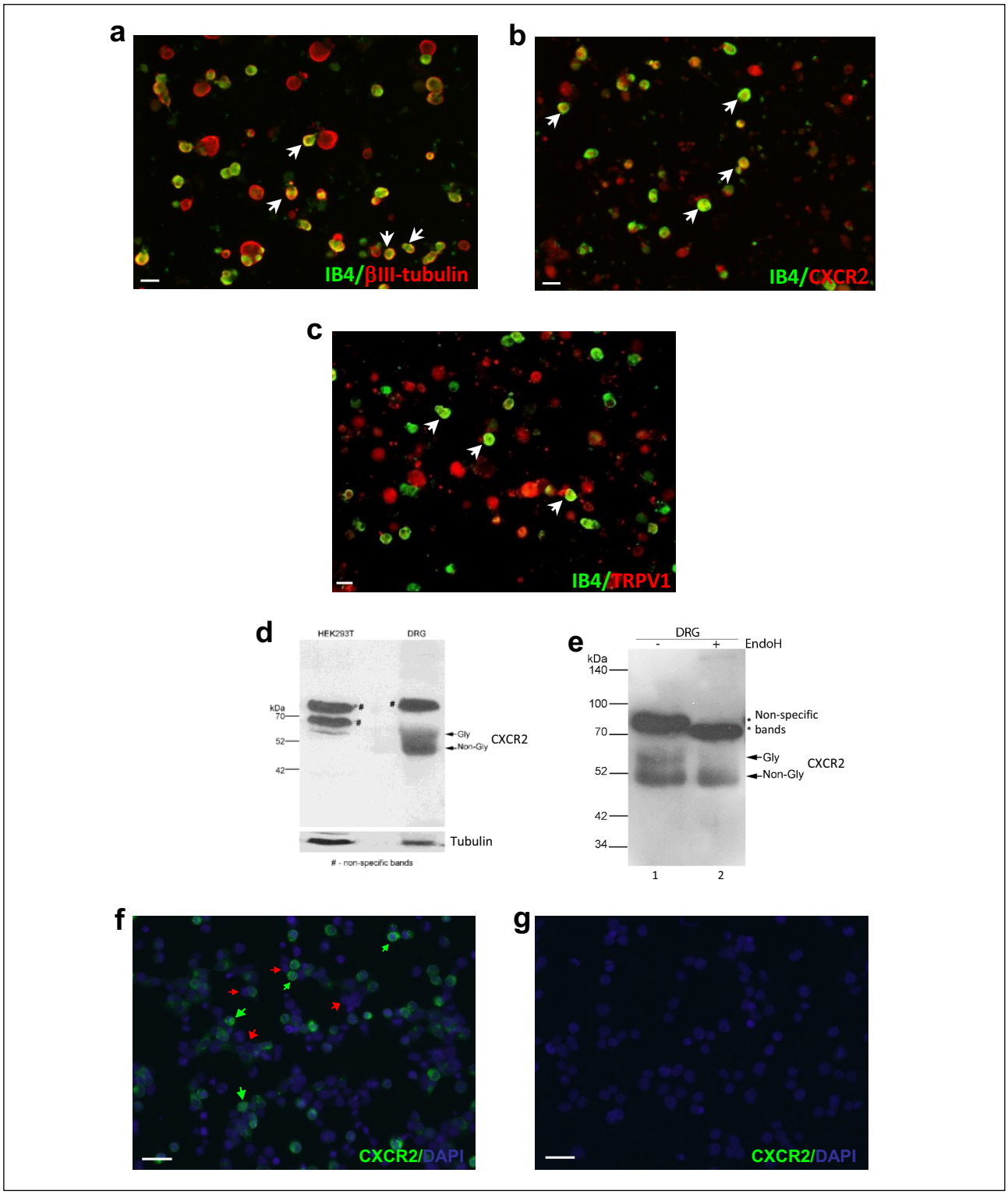

Fig. 3. CXCR2 and TRPV1 receptors are expressed in IB4$^+$ neurons. (*a*) Representative image of IB4 and βIII-tubulin immunofluorescence in DRG primary culture. Arrows points to small IB4$^+$ DRG neurons. (*b*) Representative image of IB4 and CXCR2 immunofluorescence in DRG primary culture. CXCR2 receptors are present in both IB4$^+$ and IB4$^-$ neurons. Arrows points to IB4$^+$/CXCR2$^+$ neurons. (*c*) Representative image of IB4 and TRPV1 immunofluorescence in DRG primary culture. TRPV1 receptors are present in both IB4$^+$ and IB4$^-$ neurons. Arrows points to IB4$^+$/TRPV1$^+$ neurons (scale bar for (*a*), (*b*) and (*c*) = 50 μm). (*d*) Western blot analysis for DRG and HEK293T lysates. A band corresponding to CXCR2 receptor was detected at the predicted molecular weight for the DRG sample, while no band was detected for HEK293T cells. (*e*) The glycosylation status essential for the surface expression of the receptor was also confirmed. CXCR2 was detected as both glycosylated (Gly) and non-glycosylated (Non-Gly) form, with the glycan moieties completely sensitive to glycosidase digestion (lane 2). (*f*) Representative image of CXCR2 fluorescence in HEK293T cells transiently transfected with huCXCR2 plasmid. Green arrows indicate transfected cells, and red arrows indicated non-transfected cells in which only the nucleus is stained with DAPI. (*g*) Representative image of CXCR2 fluorescence in untransfected HEK293T cells (scale bar for (*f*) and (*g*) = 25 μm).

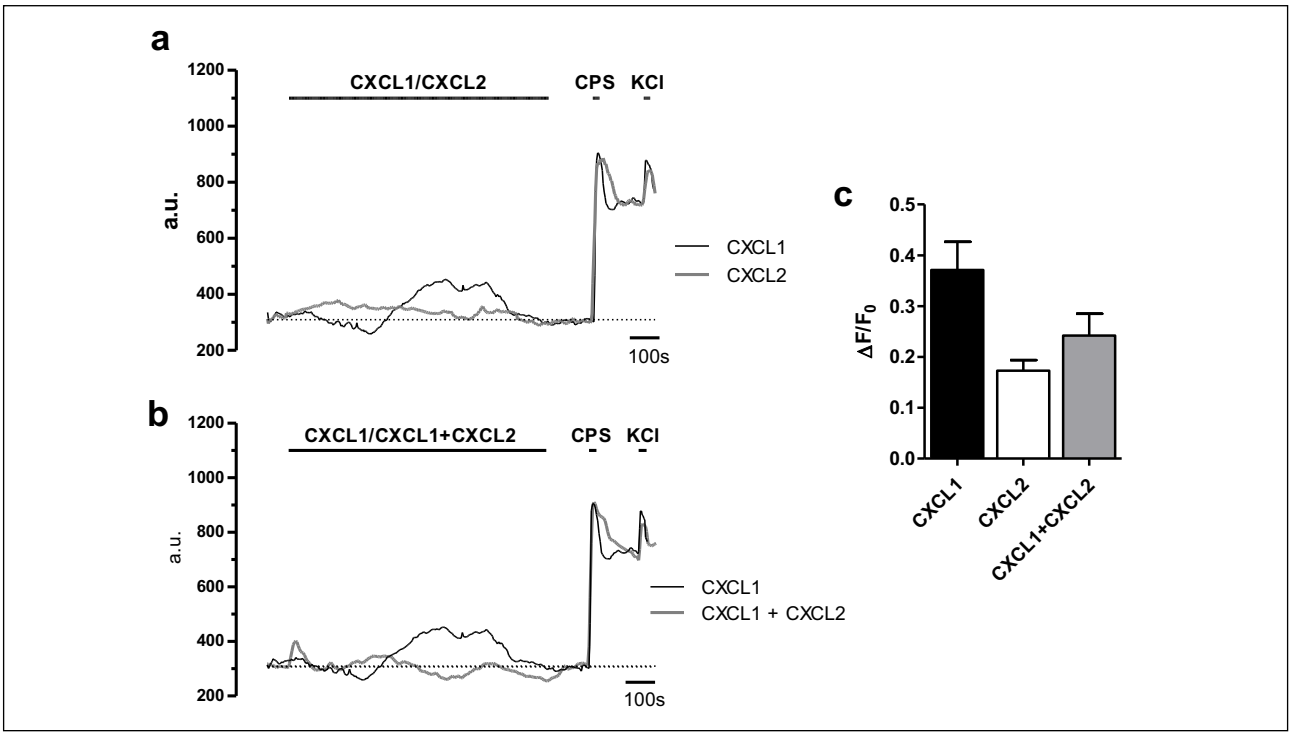

Fig. 4. Acute application of CXCL1 or CXCL2 increase $[Ca^{2+}]_i$ in different degrees. (*a*) Representative trace of $[Ca^{2+}]_i$ during 12 minutes application of CXCL1 or CXCL2, followed by 250 nM capsaicin and 50 mM KCl applications. (*b*) Representative trace of $[Ca^{2+}]_i$ during 12 minutes application of CXCL1 or CXCL1 + CXCL2, followed by 250 nM capsaicin and 50 mM KCl applications. (*c*) Bar graph of mean ΔF/F0 induced by acute application of CXCL1, CXCL2 or CXCL1 + CXCL2. CPS, capsaicin.

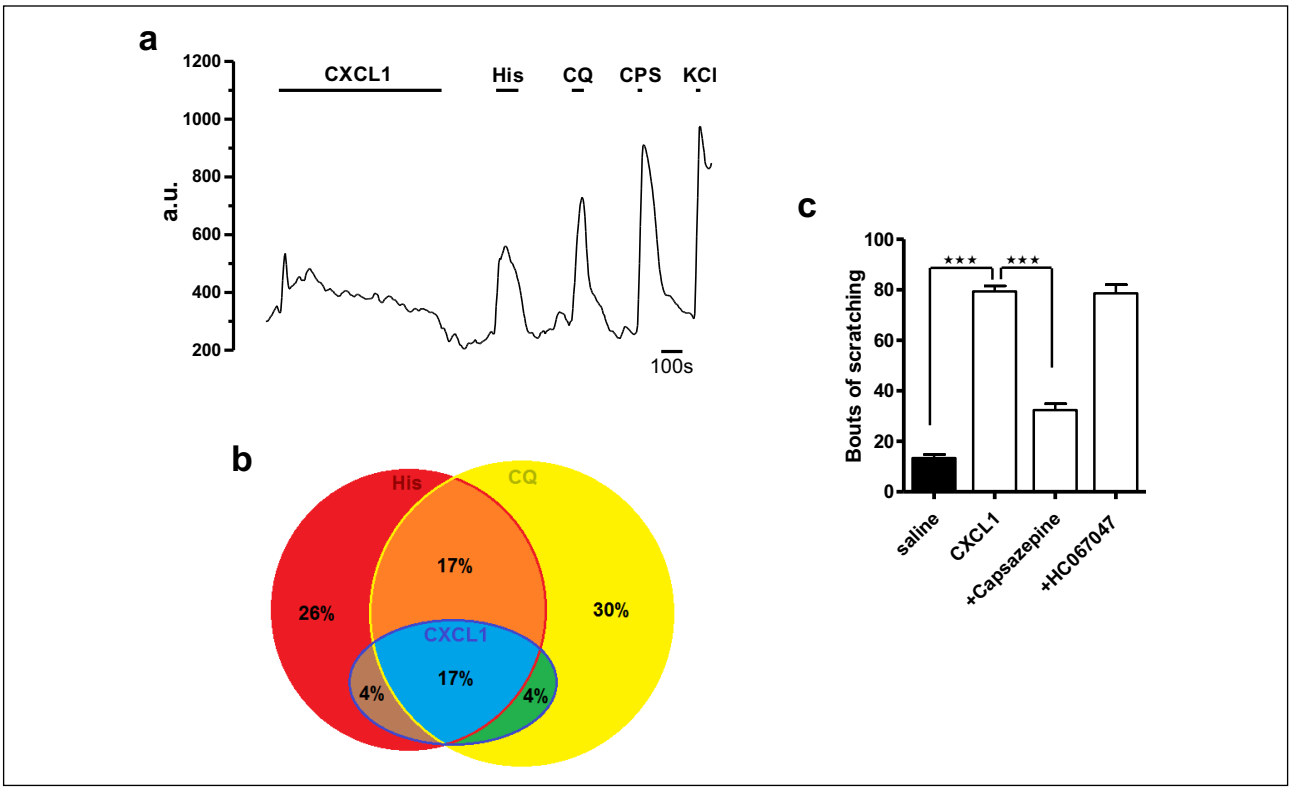

Fig. 5. CXCL1-sensitive neurons belong to a subset of itch-sensitive neurons. (*a*) Representative trace of $[Ca^{2+}]_i$ during consecutive application of CXCL1, histamine, chloroquine, capsaicin and KCl. (*b*) Diagram representing the $TRPV1^+/IB4^+$ DRG neurons that respond to one or more itch-inducing agents. The CXCL1-sensitive neurons also responded to histamine and chloroquine. (*c*) Bar graph representing bouts of scratching after intradermal injection of CXCL1 in the dorsum of the neck. CXCL1 induced a significant increase in the number of bouts of scratching compared to control animals injected with saline solution (***P < 0.001) which was significantly reduced when capsazepine was pre-injected before CXCL1 (***P < 0.001). HC067047, a TRPV4 blocker, didn't have any significant effect. His, histamine; CQ, chloroquine; CPS, capsaicin.

incubation, but when acutely applied CXCL1 activated a sub-population of itch-sensitive TRPV1$^+$/IB4$^+$ cells in a slow, low amplitude manner, while CXCL2 had a similar effect but on non-itch TRPV1$^+$/IB4$^+$ DRG neurons.

A well-known characteristic of TRPV1 functioning is that it can be sensitized or desensitized. The sensitization which occurs through protein-kinase dependent phosphorylation (29-32) is associated with higher or longer responses to specific agonists, which subsequently depolarize the neurons and increase excitability. Desensitization, which can be mediated *via* protein phosphatases dephosphorylation (33), by calmodulin interaction with TRPV1 N-terminal residues in a Ca-dependent manner (34, 35) or by IP3-induced calcium release from intracellular stores (36), is associated with reduced responses to extended or consecutive applications of capsaicin, and therefore reduced excitability. Reduced desensitization is also associated with increased excitability, because under this condition TRPV1 receptors are able to still open to new/repetitive stimuli, and thus allow depolarization. Reduced desensitization was associated with increased functioning of TRPV1 receptors after 4 hours of incubation with 1.5 nM CXCL1 chemokine (19), after overnight exposure to hypoxia/hyperglycemia specific to diabetic conditions (20) or after acute exposure to cathecolamines (37).

According to our data, CXCL1 has an activating effect on TRPV1$^+$/IB4$^+$ DRG neurons either by reducing TRPV1 desensitization after short-term incubation, or by inducing an increase in $[Ca^{2+}]_i$ which further on depolarizes the cells and increases excitability at acute application. The activation by reducing TRPV1 desensitization was a concentration dependent effect visible in the whole TRPV1$^+$/IB4$^+$ population that was selected for analysis, while the activation by increasing $[Ca^{2+}]_i$ was elicited in only 23% of TRPV1$^+$/IB4$^+$ cells. The cells activated by acute application of CXCL1 also responded to itch-inducing agents, histamine and chloroquine (*Fig*. *5b*), suggesting that they most likely belong to the itch-sensitive DRG neurons sub-population. Therefore, CXCL1 may activate the CXCL1-sensitive, itch-sensitive population through both increasing $[Ca^{2+}]_i$ (acute application) and reducing TRPV1 desensitization (short-term incubation), while in the rest of the TRPV1$^+$/IB4$^+$ population CXCL1 only reduces TRPV1 desensitization (short-term incubation) with other possible consequences, like pain sensitivity. Our data suggest a mechanism for the itch-inducing effects of CXCL1 (4, 5, 38) and additionally characterize the mechanism of nociceptor activation by CXCL1 *via* reduced TRPV1 desensitization at short-term application (19). Beside this mechanism, CXCL1 can induce pain by potentiating NMDA-induced currents (39) or by increasing ERK (extracellular signal-regulated kinase) and CREB (cAMP response element binding protein) signaling pathways in spinal cord neurons (40).

In contrast to CXCL1, CXCL2 seems to mainly activate the non-itch sensitive TRPV1$^+$/IB4$^+$ DRG neurons, more by reducing TRPV1 desensitization which is similar to the one induced by CXCL1, and less by increasing $[Ca^{2+}]_i$ which is lower than the one induced by CXCL1 and exhibited by a smaller population of cells. This mechanisms could explain the pain inducing effects of CXCL2 besides hyperacetylation of histone H3 on its promoter region, an effect known to elicit chronic neuroinflammation (41).

The possibility that CXCL1 and CXCL2 could act on other TRPV1$^+$/IB4$^+$ non-itch sensitive cells is also supported by our ICC results and data from the literature (42), showing that CXCR2 receptors are expressed in all DRG neurons, not in only a subset of IB4$^+$ neurons.

In previous studies, we showed that at long-term incubation CXCL1 and CXCL2 have opposite effects on TRPV1 (3), which cumulated with our present data offer an interesting picture about how these two chemokines might act on DRG neurons. CXCL1 has a slow, low amplitude activating effect at acute application by increasing $[Ca^{2+}]_i$ in an itch-sensitive subset of DRG neurons, after short-term incubation activates all TRPV1$^+$/IB4$^+$ DRG neurons by reducing TRPV1 desensitization, while after long-term incubation its influence on TRPV1 disappears (3). CXCL2 has a smaller activating effect at acute application mainly on a non-itch subset of DRG neurons, after short-term incubation has the same activating effect like CXCL1, while after long-term incubation it starts to inhibit the TRPV1 receptors (3). The most intriguing is of course CXCL2 which on short-term activates and on long-term inhibits DRG neurons, suggesting a highly complex and diverse signaling pathways mediated by CXCR2 receptors.

CXCR2 is a seven transmembrane G-protein coupled receptor (GPCR) that functions as a dimer and is activated by all seven ELR (+) CXC-chemokines (CXCL1-3 and CXCL5-8) (2, 43). Upon ligand binding, the receptor couples to $G_{i/o}$ protein and activates several protein kinase pathways (19, 25, 44, 45) that can induce diverse intracellular effects, including CXCR2 phosphorylation followed by desensitization (46). In addition, in the first 2 – 10 minutes of their activation 95% of the receptors are desensitized even more due to a dose-dependent internalization process followed by recovery to the membrane, degradation or initiation of post-internalization signaling (47, 48). The post internalization signals are possible because CXCR2 forms dynamic and temporal assembly with other adaptor signaling proteins through which it can initiate other intracellular pathways (49). Therefore, it is highly possible that the antagonistic effects of CXCL2 are due to the complex functioning of CXCR2 receptors and its downstream activation of different signaling pathways.

Data about different time-dependent effects mediated by distinct signaling pathways are available for both CXCL2 and CXCL1. Apoptotic death of hippocampal neurons *via* caspase 1, 3 and Gαi signaling pathways was described after short-term exposure (4 h) to CXCL2, in the same nanomolar range as in our study (50). It is known that over-activated TRPV1 receptors induce calcium-dependent apoptosis (51), therefore it is possible that TRPV1 activation by the mechanism we described in our study and which occurs in the same time range as the data mentioned above, to be also involved in the apoptotic effects of CXCL2 on hippocampal neurons. In contrast, long-term exposure to CXCL2 (24 – 48 h to days) has neuroprotective effects on hippocampal and cerebral neurons by activating MEK1-ERK1/2 and PI3K-Akt signaling pathways, by suppressing the mislocalization of p21-activated kinase (PAK) or by stimulating astrocytes-derived bFGF (basic fibroblast growth factor) (50, 52, 53). Recent data showed that blocking TRPV1 receptors before a sciatic nerve injury accelerates regeneration (54), or that its inhibition 3 hours after stroke significantly reduced the infarct volume and conferred neuroprotection (55). Given the fact that we observed that on long-term CXCL2 has an inhibitory effect on both the amplitude and desensitization rate of TRPV1 current, it could be possible that the neuroprotective effects of CXCL2 on hippocampal and cerebral neurons to be also due to reducing TRPV1 activation. For CXCL1, data on short-term (h) exposure are associated with pain sensitivity due to reduced TRPV1 desensitization in DRG neurons (19), similar to our data, or to increased release of CGRP which contributes to neurogenic inflammation (25). On long-term (24 – 48 h) CXCL1 continues to produce pain by activating Na_v or K_v channels in the DRG neurons (26, 42), not TRPV1 as our previous data also showed (3). On long-term CXCL1 also contributes to brain development by promoting proliferation of early oligodendrocyte progenitor cells acting through an ERK1/2-dependent pathway and through release of IL-6 from astrocytes (56) and even has analgesic effects by stimulating secretion of opioids by granulocytes (57). These data reinforce our observations that even though CXCL1 and

CXCL2 share a 78% homology of their sequence they could have distinct, even antagonistic effects.

An interesting observation was that CXCL2 can reduce CXCL1 effect when acting together. According to the existing data, both CXCL1 and CXCL2 bind to CXCR2 receptors with high affinity on a binding site located on the extracellular site, in a two-steps process described as the 'fly-casting mechanism' (2, 58-60). The maximal binding of CXCL1 to CXCR2 is dependent on the presence on the cell surface of heparan sulfate proteoglycans and can be reduced by CXCL10 chemokine which interferes with CXCL1 binding to heparan sulfate (61). Possibly, the inhibitory effect of CXCL2 on CXCL1 is mediated by a similar mechanism, but at this step there are not enough experimental data to support such a mechanism.

If reducing TRPV1 desensitization in $IB4^+$ DRG neurons is a clear effect for both CXCL1 and CXCL2 upon short-term incubation, the mechanism of increasing $[Ca^{2+}]_i$ by the two chemokines is not equally clear. This could be due to TRP channels activation, most likely TRPV1 as suggested by the behavioral studies in which the pretreatment with capsazepine significantly reduced the scratch behavior induced by CXCL1. Intradermal injection in the nape of the neck of pruritogens is frequently used to investigate itch (23, 62), although it has been suggested that in this model scratching could also be a response to pain, besides itch (63, 64). In our case, most likely, CXCL1 activated upon injection all CXCR2-expressing $TRPV1^+/IB4^+$ DRG neurons, including the itch- and non-itch-sensitive cells. Since the pre-treatment with capsazepine significantly reduced the bouts of scratching, and the bouts of scratching are considered an important indicator of the magnitude of itch-related scratching (23), we may conclude that an important part of the scratching-induced response of CXCL1 upon injection in the nape of the neck is due to an itch-component, which is highly possible to be mediated by TRPV1.

Another candidate for the CXCL1-induced $[Ca^{2+}]_i$ increase could also be TRPA1 since it has been shown to be an essential downstream effector of chloroquine and BAM-22 (9) and in our experiments 21% of CXCL1 sensitive cells also responded to chloroquine. A potential TRPA1 contribution might also be relevant for other itch-associated disease, like diabetes, frequently associated with pruritus in the initial stages (65). Cutaneous application of methylglyoxal, a reactive carbonyl compound generated in diabetes mellitus, is known to have pronociceptive effects by TRPA1 activation (66), but it may also contribute to increased pruritus *via* a putative activation of TRPA1 receptors by CXCL1, known to be secreted by AGEs (advanced glycoxylation end products)-activated skin macrophages in diabetes (67-69).

In addition, other sources of Ca^{2+} should also be considered, since previous studies have shown that acute application of CXCL1 can induce an increase in $[Ca^{2+}]_i$ associated with CGRP release in neonatal rat DRG neurons (25) or with an enhancement of the neurotransmitter release in mice Purkinje neurons (70) *via* N-type Ca_v channels of *via* intracellular ryanodine-sensitive or IP3 (inositol 1,4,5 trisphosphate)-sensitive calcium stores. Given all these possible sources for Ca^{2+}, additional experiments will be required to clarify the mechanism.

In conclusion, this study brings new data about the mechanism of action on $TRPV1^+/IB4^+$ DRG neurons of CXCL1 and CXCL2 chemokines after short-term (4 h) incubation or acute (12 minutes) application. The results showed that after short-term incubation both chemokines can activate $TRPV1^+/IB4^+$ DRG neurons by significantly reducing TRPV1 desensitization, while at acute application both chemokines induced an increase in $[Ca^{2+}]_i$ although of different amplitudes, in a subset of neurons partially also itch-sensitive in the case of CXCL1, or non-itch sensitive in the case of CXCL2. The short-term experiments bring additional information about a pain inducing mechanism of CXCL1 and reveal a new mechanism of activating DRG nociceptors by CXCL2. The acute experiments suggested a mechanism of action for the itch-inducing effect of CXCL1 and offered an explanation for the lack of itch-inducing effects of CXCL2 even though it shares 78% homology with CXCL1. Additional experiments will be required to clarify in more details how CXCL1 activates the itch-sensitive subset of $TRPV1^+/IB4^+$ DRG neurons for a more efficient therapeutic approach of pruritus associated with atopic dermatitis.

Abbreviations: BAM8-22 peptide, bovine adrenal medulla 8-22 peptide; $[Ca^{2+}]_i$, intracellular calcium concentration; Ca_v, voltage-gated Ca^{2+} channels; CGRP, calcitonin gene-related peptide; CPS, capsaicin; CQ, chloroquine; CREB, cAMP response element binding protein; CXCL1, chemokine (C-X-C motif) ligand 1; CXCL2, chemokine (C-X-C motif) ligand 2; CXCL10, chemokine (C-X-C motif) ligand 10; CXCR2, (C-X-C motif) receptor 2; DAPI, 4',6-diamidino-2-phenylindole; DMEM, Dulbecco's Modified Eagle Medium; DMSO, dimethyl sulfoxide; DRG, dorsal root ganglia; DTT, dithiothreitol; EndoH, endoglycosidase H; ERK, extracellular signal-regulated kinase; ES, extracellular solution; FITC, fluorescein isothiocyanate; Gly, glycosylated; GPCR, G-protein coupled receptor; HEK293T, human embryonic kidney cells; His, histamine; HRP, horse radish peroxidase; IB4, isolectin B4; ICC, immunocytochemistry; IL-31, interleukin 31; IP3, inositol 1,4,5 trisphosphate; MrgprA3, Mas-related G-protein coupled receptor A3; MrgprC11, Mas-related G-protein coupled receptor C11; NGF, nerve growth factor; NMDA, N-methyl-D-aspartate; PBS, phosphate buffered saline; PFA, paraformaldehyde; PKC, protein kinase C; PLC, phospholipase C; RIPA buffer, radioimmunoprecipitation assay buffer; SDS, sodium dodecyl sulfate; TRP, transient receptor potential; TRPA1, transient receptor potential channel subfamily A member 1; TRPV1, transient receptor potential vanilloid type 1 channel; TRPV4, transient receptor potential vanilloid type 4 channel

Acknowledgements: A.F. Deftu and A. Filippi contributed equally to this work. We greatly appreciate Dr. Stefana Petrescu from the Institute of Biochemistry for valuable discussions and to Cornelia Dragomir, Geanina Haralambie and Antonia-Teona Deftu from University of Bucharest for technical support. This research was funded by the Romanian Government *via* UEFISCDI (Executive Unit for Higher Education, Research, Development and Innovation Funding) grant 205/2014 awarded to V.R. and by the Ministry of Education, Culture, Sports, Science and Technology from Japan through projects 15H05934 (Thermal Biology), 24111507+26111702 (Brain Environment) and 26117502 (Glial assembly) awarded to K.S. under the program Grants-in-Aid for Scientific Research.

Conflict of interests: None declared.

REFERENCES

1. Semple BD, Kossmann T, Morganti-Kossmann MC. Role of chemokines in CNS health and pathology: a focus on the CCL2/CCR2 and CXCL8/CXCR2 networks. *J Cereb Blood Flow Metab* 2010; 30: 459-473.
2. Veenstra M, Ransohoff RM. Chemokine receptor CXCR2: physiology regulator and neuroinflammation controller? *J Neuroimmunol* 2012; 246: 1-9.
3. Deftu A, Deftu A, Ristoiu V. Long-term incubation with CXCL2, but not with CXCL1, alters the kinetics of TRPV1 receptors in cultured DRG neurons. *Arch Biol Sci* 2016; 69: 74. doi: 10.2298/ABS160513074D

4. Cheung PF, Wong CK, Ho AW, Hu S, Chen DP, Lam CW. Activation of human eosinophils and epidermal keratinocytes by Th2 cytokine IL-31: implication for the immunopathogenesis of atopic dermatitis. *Int Immunol* 2010; 22: 453-467.
5. Kalish H, Phillips TM. Assessment of chemokine profiles in human skin biopsies by an immunoaffinity capillary electrophoresis chip. *Methods* 2012; 56: 198-203.
6. Ikoma A, Steinhoff M, Stander S, Yosipovitch G, Schmelz M. The neurobiology of itch. *Nat Rev Neurosci* 2006; 7: 535-547.
7. Ross SE. Pain and itch: insights into the neural circuits of aversive somatosensation in health and disease. *Curr Opin Neurobiol* 2011; 21: 880-887.
8. Imamachi N, Park GH, Lee H, *et al*. TRPV1-expressing primary afferents generate behavioral responses to pruritogens via multiple mechanisms. *Proc Nat Acad Sci USA* 2009; 106: 11330-11335.
9. Wilson SR, Gerhold KA, Bifolck-Fisher A, *et al*. TRPA1 is required for histamine-independent, Mas-related G protein-coupled receptor-mediated itch. *Nat Neurosci* 2011; 14: 595-602.
10. Kittaka H, Tominaga M. The molecular and cellular mechanisms of itch and the involvement of TRP channels in the peripheral sensory nervous system and skin. *Allergol Int* 2017; 66: 22-30.
11. Han SK, Mancino V, Simon MI. Phospholipase Cbeta 3 mediates the scratching response activated by the histamine H1 receptor on C-fiber nociceptive neurons. *Neuron* 2006; 52: 691-703.
12. Valtcheva MV, Davidson S, Zhao C, Leitges M, Gereau RW. Protein kinase Cdelta mediates histamine-evoked itch and responses in pruriceptors. *Mol Pain* 2015; 11: 1. doi: 10.1186/1744-8069-11-1
13. Liu Q, Tang Z, Surdenikova L, *et al*. Sensory neuron-specific GPCR Mrgprs are itch receptors mediating chloroquine-induced pruritus. *Cell* 2009; 139: 1353-1365.
14. Dong X, Han S, Zylka MJ, Simon MI, Anderson DJ. A diverse family of GPCRs expressed in specific subsets of nociceptive sensory neurons. *Cell* 2001; 106: 619-632.
15. Cevikbas F, Wang X, Akiyama T, *et al*. A sensory neuron-expressed IL-31 receptor mediates T helper cell-dependent itch: Involvement of TRPV1 and TRPA1. *J Allergy Clin Immunol* 2014; 133: 448-460.
16. Shim WS, Tak MH, Lee MH, *et al*. TRPV1 mediates histamine-induced itching via the activation of phospholipase A2 and 12-lipoxygenase. *J Neurosci* 2007; 27: 2331-2337.
17. Vriens J, Appendino G, Nilius B. Pharmacology of vanilloid transient receptor potential cation channels. *Mol Pharmacol* 2009; 75: 1262-1279.
18. Tominaga M, Caterina MJ, Malmberg AB, *et al*. The cloned capsaicin receptor integrates multiple pain-producing stimuli. *Neuron* 1998; 21: 531-543.
19. Dong F, Du YR, Xie W, Strong JA, He XJ, Zhang JM. Increased function of the TRPV1 channel in small sensory neurons after local inflammation or in vitro exposure to the pro-inflammatory cytokine GRO/KC. *Neurosci Bull* 2012; 28: 155-164.
20. Ristoiu V, Shibasaki K, Uchida K, *et al*. Hypoxia-induced sensitization of transient receptor potential vanilloid 1 involves activation of hypoxia-inducible factor-1 alpha and PKC. *Pain* 2011; 152: 936-945.
21. Stucky CL, Lewin GR. Isolectin B(4)-positive and -negative nociceptors are functionally distinct. *J Neurosci* 1999; 19: 6497-6505.
22. Marin MB, Ghenea S, Spiridon LN, Chiritoiu GN, Petrescu AJ, Petrescu SM. Tyrosinase degradation is prevented when EDEM1 lacks the intrinsically disordered region. *PloS One* 2012; 7: e42998. doi: 10.1371/journal.pone.0042998.
23. Nojima H, Carstens E. Quantitative assessment of directed hind limb scratching behavior as a rodent itch model. *J Neurosci Methods* 2003; 126: 137-143.
24. Dirajlal S, Pauers LE, Stucky CL. Differential response properties of IB(4)-positive and -negative unmyelinated sensory neurons to protons and capsaicin. *J Neurophysiol* 2003; 89: 513-424.
25. Qin X, Wan Y, Wang X. CCL2 and CXCL1 trigger calcitonin gene-related peptide release by exciting primary nociceptive neurons. *J Neurosci Res* 2005; 82: 51-62.
26. Yang RH, Strong JA, Zhang JM. NF-kappaB mediated enhancement of potassium currents by the chemokine CXCL1/growth related oncogene in small diameter rat sensory neurons. *Mol Pain* 2009; 5: 26. doi: 10.1186/1744-8069-5-26
27. Bhardwaj D, Nager M, Camats J, *et al*. Chemokines induce axon outgrowth downstream of hepatocyte growth factor and TCF/beta-catenin signaling. *Front Cell Neurosci* 2013; 7: 52. doi: 10.3389/fncel.2013.00052
28. Mayer AM, Murphy J, MacAdam D, *et al*. Classical and alternative activation of cyanobacterium oscillatoria sp. lipopolysaccharide-treated rat microglia in vitro. *Toxicol Sci* 2016; 149: 484-495.
29. De Petrocellis L, Harrison S, Bisogno T, *et al*. The vanilloid receptor (VR1)-mediated effects of anandamide are potently enhanced by the cAMP-dependent protein kinase. *J Neurochem* 2001; 77: 1660-1663.
30. Premkumar LS, Ahern GP. Induction of vanilloid receptor channel activity by protein kinase C. *Nature* 2000; 408: 985-990.
31. Price TJ, Jeske NA, Flores CM, Hargreaves KM. Pharmacological interactions between calcium/calmodulin-dependent kinase II alpha and TRPV1 receptors in rat trigeminal sensory neurons. *Neurosci Lett* 2005; 389: 94-98.
32. Tominaga M, Tominaga T. Structure and function of TRPV1. *Pflugers Arch* 2005; 451: 143-150.
33. Docherty RJ, Yeats JC, Bevan S, Boddeke HW. Inhibition of calcineurin inhibits the desensitization of capsaicin-evoked currents in cultured dorsal root ganglion neurones from adult rats. *Pflugers Arch* 1996; 431: 828-837.
34. Numazaki M, Tominaga T, Takeuchi K, Murayama N, Toyooka H, Tominaga M. Structural determinant of TRPV1 desensitization interacts with calmodulin. *Proc Nat Acad Sci USA* 2003; 100: 8002-8006.
35. Rosenbaum T, Gordon-Shaag A, Munari M, Gordon SE. Ca^{2+}/calmodulin modulates TRPV1 activation by capsaicin. *J Gen Physiol* 2004; 123: 53-62.
36. Hucho T, Suckow V, Joseph EK, *et al*. Ca^{++}/CaMKII switches nociceptor-sensitizing stimuli into desensitizing stimuli. *J Neurochem* 2012; 123: 589-601.
37. Filippi A, Caruntu C, Gheorghe RO, Deftu A, Amuzescu B, Ristoiu V. Catecholamines reduce TRPV1 desensitization in cultured dorsal root ganglia neurons. *J Physiol Pharmacol* 2016; 67: 843-850.
38. Chang KT, Lin HY, Kuo CH, Hung CH. Tacrolimus suppresses atopic dermatitis-associated cytokines and chemokines in monocytes. *J Microbiol Immunol Infect* 2016; 49: 409-416.
39. Cao DL, Zhang ZJ, Xie RG, Jiang BC, Ji RR, Gao YJ. Chemokine CXCL1 enhances inflammatory pain and increases NMDA receptor activity and COX-2 expression in spinal cord neurons via activation of CXCR2. *Exp Neurol* 2014; 261: 328-336.
40. Zhang ZJ, Cao DL, Zhang X, Ji RR, Gao YJ. Chemokine contribution to neuropathic pain: respective induction of

CXCL1 and CXCR2 in spinal cord astrocytes and neurons. *Pain* 2013; 154: 2185-2197.
41. Kiguchi N, Kobayashi Y, Maeda T, *et al*. Epigenetic augmentation of the macrophage inflammatory protein 2/C-X-C chemokine receptor type 2 axis through histone H3 acetylation in injured peripheral nerves elicits neuropathic pain. *J Pharmacol Exp Ther* 2012; 340: 577-587.
42. Wang JG, Strong JA, Xie W, *et al*. The chemokine CXCL1/growth related oncogene increases sodium currents and neuronal excitability in small diameter sensory neurons. *Mol Pain* 2008; 4: 38. doi: 10.1186/1744-8069-4-38
43. Trettel F, Di Bartolomeo S, Lauro C, Catalano M, Ciotti MT, Limatola C. Ligand-independent CXCR2 dimerization. *J Biol Chem* 2003; 278: 40980-40988.
44. Guo H, Liu Z, Xu B, *et al*. Chemokine receptor CXCR2 is transactivated by p53 and induces p38-mediated cellular senescence in response to DNA damage. *Aging Cell* 2013; 12: 1110-1121.
45. Wang S, Wu Y, Hou Y, *et al*. CXCR2 macromolecular complex in pancreatic cancer: a potential therapeutic target in tumor growth. *Transl Oncol* 2013; 6: 216-225.
46. Raghuwanshi SK, Su Y, Singh V, Haynes K, Richmond A, Richardson RM. The chemokine receptors CXCR1 and CXCR2 couple to distinct G protein-coupled receptor kinases to mediate and regulate leukocyte functions. *J Immunol* 2012; 189: 2824-2832.
47. Nasser MW, Raghuwanshi SK, Malloy KM, *et al*. CXCR1 and CXCR2 activation and regulation. Role of aspartate 199 of the second extracellular loop of CXCR2 in CXCL8-mediated rapid receptor internalization. *J Biol Chem* 2007; 282: 6906-6915.
48. Rose JJ, Foley JF, Murphy PM, Venkatesan S. On the mechanism and significance of ligand-induced internalization of human neutrophil chemokine receptors CXCR1 and CXCR2. *J Biol Chem* 2004; 279: 24372-24386.
49. Raman D, Neel NF, Sai J, Mernaugh RL, Ham AJ, Richmond AJ. Characterization of chemokine receptor CXCR2 interacting proteins using a proteomics approach to define the CXCR2 'chemosynapse'. *Methods Enzymol* 2009; 460: 315-330.
50. Kalehua AN, Nagel JE, Whelchel LM, *et al*. Monocyte chemoattractant protein-1 and macrophage inflammatory protein-2 are involved in both excitotoxin-induced neurodegeneration and regeneration. *Exp Cell Res* 2004; 297: 197-211.
51. Ho KW, Ward NJ, Calkins DJ. TRPV1: a stress response protein in the central nervous system. *Am J Neurodegener Dis* 2012; 1: 1-14.
52. Raman D, Milatovic SZ, Milatovic D, Splittgerber R, Fan GH, Richmond A. Chemokines, macrophage inflammatory protein-2 and stromal cell-derived factor-1alpha, suppress amyloid beta-induced neurotoxicity. *Toxicol Appl Pharmacol* 2011; 256: 300-313.
53. Watson K, Fan GH. Macrophage inflammatory protein 2 inhibits beta-amyloid peptide (1-42)-mediated hippocampal neuronal apoptosis through activation of mitogen-activated protein kinase and phosphatidylinositol 3-kinase signaling pathways. *Mol Pharmacol* 2005; 67: 757-765.
54. Ren F, Zhang H, Qi C, Gao ML, Wang H, Li XQ. Blockade of transient receptor potential cation channel subfamily V member 1 promotes regeneration after sciatic nerve injury. *Neural Regen Res* 2015; 10: 1324-1331.
55. Hakimizadeh E, Shamsizadeh A, Roohbakhsh A, *et al*. Inhibition of transient receptor potential vanilloid-1 confers neuroprotection, reduces tumor necrosis factor-alpha, and increases IL-10 in a rat stroke model. *Fundam Clin Pharmacol* 2017; Feb. 15. doi: 10.1111/fcp.12279 [epub ahead of print].
56. Filipovic R, Zecevic N. The effect of CXCL1 on human fetal oligodendrocyte progenitor cells. *Glia* 2008; 56: 1-15.
57. Rittner HL, Brack A, Stein C. The other side of the medal: how chemokines promote analgesia. *Neurosci Lett* 2008; 437: 203-208.
58. Rajasekaran D, Keeler C, Syed MA, *et al*. A model of GAG/MIP-2/CXCR2 interfaces and its functional effects. *Biochemistry* 2012; 51: 5642-5654.
59. Ravindran A, Sawant KV, Sarmiento J, Navarro J, Rajarathnam K. Chemokine CXCL1 dimer is a potent agonist for the CXCR2 receptor. *J Biol Chem* 2013; 288: 12244-12252.
60. Scholten DJ, Canals M, Maussang D, *et al*. Pharmacological modulation of chemokine receptor function. *Brit J Pharmacol* 2012; 165: 1617-1643.
61. Wang D, Sai J, Richmond A. Cell surface heparan sulfate participates in CXCL1-induced signaling. *Biochemistry* 2003; 42: 1071-1077.
62. Cowan A, Lyu RM, Chen YH, Dun SL, Chang JK, Dun NJ. Phoenixin: a candidate pruritogen in the mouse. *Neuroscience* 2015; 310: 541-548.
63. Shimada SG, LaMotte RH. Behavioral differentiation between itch and pain in mouse. *Pain* 2008; 139: 681-687.
64. Spradley JM, Davoodi A, Carstens MI, Carstens E. Effects of acute stressors on itch- and pain-related behaviors in rats. *Pain* 2012; 153: 1890-1897.
65. Bustan RS, Wasim D, Yderstraede KB, Bygum A. Specific skin signs as a cutaneous marker of diabetes mellitus and the prediabetic state - a systematic review. *Dan Med J* 2017; 64: A5316.
66. Viisanen H, Chapman H, Wei H, *et al*. Pronociceptive effects induced by cutaneous application of a transient receptor potential ankyrin 1 (TRPA1) channel agonist methylglyoxal in diabetic animals: comparison with tunicamycin-induced endoplastic reticulum stress. *J Physiol Pharmacol* 2016; 67: 587-594.
67. Diana J, Lehuen A. Macrophages and beta-cells are responsible for CXCR2-mediated neutrophil infiltration of the pancreas during autoimmune diabetes. *EMBO Mol Med* 2014; 6: 1090-1104.
68. Maessen DE, Stehouwer CD, Schalkwijk CG. The role of methylglyoxal and the glyoxalase system in diabetes and other age-related diseases. *Clin Sci* 2015; 128: 839-861.
69. Jin X, Yao T, Zhou Z, *et al*. Advanced glycation end products enhance macrophages polarization into M1 phenotype through activating RAGE/NF-kappaB pathway. *Biomed Res Int* 2015; 2015: 732450. doi: 10.1155/2015/732450
70. Giovannelli A, Limatola C, Ragozzino D, *et al*. CXC chemokines interleukin-8 (IL-8) and growth-related gene product alpha (GROalpha) modulate Purkinje neuron activity in mouse cerebellum. *J Neuroimmunol* 1998; 92: 122-132.

Received: February 24, 2017
Accepted: May 31, 2017

Author's address: Prof. Violeta Ristoiu, Splaiul Independentei 91-95, 050095, Bucharest, Romania.
E-mail: v_ristoiu@yahoo.com